Title

Excitation Gap in the Kondo Insulator with Coulomb Interaction between Conduction Electrons

Author(s)

Aya Masuyama and Tetsuya Mutou

Journal

Journal of the Physical Society of Japan vol.89, No.4

Published

2020-03-23

URL

https://doi.org/10.7566/JPSJ.89.044708

Excitation Gap in the Kondo Insulator with Coulomb Interaction between Conduction Electrons

Aya Masuyama and Tetsuya Mutou*

Interdisciplinary Faculty of Science and Engineering, Shimane University, Matsue 690-8504, Japan

We have investigated the effects of the Coulomb interaction between conduction electrons on the excitation gap of the Kondo insulator . As a theoretical model of the Kondo insulator, the periodic Anderson model (PAM) has been used under particle-hole symmetry. We have treated the PAM with the Coulomb interaction between the conduction electrons, denoted by U_c, using the dynamic mean-field theory (DMFT) with the iterated perturbation theory as the DMFT impurity solver. With increasing U_c, the gap of the density of states at absolute zero widens and the characteristic temperature at which the electronic state begins to be reconstructed increases. We have found, via the perturbative approach, that the gap in the theoretical model of the Kondo insulator is widened by U_c, at least in the weak-coupling regime.

1. Introduction

The Kondo insulator is one of the heavy fermion systems, and the origin of the Kondo insulator excitation gap has attracted significant interest.[1,2] Although it has been established that the characteristic electronic states of the heavy fermion systems originate from the strong correlation between almost localized f electrons that hybridize with conduction electrons,[3] there are various views with regard to the origin of the Kondo insulator gap. In one view, the Kondo insulator gap is considered as an open hybridization gap in the renormalized hybridization band consisting of f electrons and conduction electrons.[4,5] The renormalized hybridization band in heavy fermions is theoretically described by the periodic Anderson model (PAM).[3] In contrast, when considering almost localized f electrons as having completely localized spins in heavy fermion systems, the theoretical model suitable for describing such a situation is the Kondo lattice model (KLM). In the KLM, a localized f spin couples with a

---

*tmutou@riko.shimane-u.ac.jp

spin of a conduction electron at the same site via the antiferromagnetic exchange interaction between them. The KLM is an effective low-energy model of the PAM in the case that the Coulomb interaction energy between f electrons is sufficiently greater than the hybridization energy of the PAM. In studies on the one-dimensional KLM, it was pointed out that the KLM excitation gap in the strong-coupling limit is understood as the spin excitation gap of the singlet state between a localized f spin and a spin of a conduction electron on the same site. Moreover, it was reported that both spin- and charge-excitation gaps exist for any exchange coupling strength.[6,7]

In the PAM, the hybridization gap becomes small when the Coulomb interaction between f electrons is strong and/or the hybridization energy is small.[4,5] It was also reported in KLM studies that the excitation gap decreases when the exchange interaction energy decreases.[6,7] In the case of such a small gap, it should no longer be valid to neglect the Coulomb interaction between conduction electrons; however, this is usually neglected in both models. The effect of the Coulomb interaction between conduction electrons, denoted here by U_c, has been already studied in both KLM[8] and PAM.[9] However, there was a discrepancy in the effect of U_c on the gap between the former and the latter.

In the numerical study of the one-dimensional KLM with U_c by the density-matrix renormalization-group (DMRG) method, it was shown that the excitation gap increases with the increase of U_c.[8] One the other hand, in the numerical study of the PAM with U_c by the Gutzwiller variational method, it was reported that switching U_c tends to reduce the gap in the PAM.[9] As the models used in these two studies are different, discrepancies in the results are expected. Nevertheless, since the KLM is an effective model of PAM with some limiting cases mentioned above, these two models should have common features in the low-energy excitation, including the excitation gap. Therefore, it is expected that there will be some common points about the effect of U_c on the excitation gap in both models.

To consider the cause of the discrepancies between the above two studies, the Coulomb interaction between f electrons, denoted here by U_f, in the PAM should be noted. In Ref. 9, the authors took the strongly asymmetric case with the infinite U_f and the sufficiently deep f level in the PAM, i.e., they considered the PAM in the subspace excluded the double occupancy of f electrons in a single site. Although KLM is considered to be a low-energy effective model of PAM in the above subspace, it is not a trivial problem whether the effect of U_c on the gap in the PAM with a *finite* value of U_f is the same as that with an *infinite* U_f or not.

In the present study, we investigate the effect of U_c on the hybridization gap in PAM with the *finite* value of U_f to reveal the cause of the discrepancy between the results obtained in Refs. 8 and 9. Specifically, we address the correlation effect on the gap opened in the density of states of the system. In the present study, the dynamic mean-field theory (DMFT) is used to treat the correlation effect in the model. DMFT is one of the established methods to treat the correlation effect in the strongly correlated electron systems.[10] DMFT is expected to be useful in investigating the correlation effects caused by both U_f and U_c on the same footing. Moreover, quantitative results can be obtained in the weak-coupling regime described by the perturbative approach with the use of the iterated perturbation theory (IPT) as the DMFT impurity solver.[11] To estimate the hybridization gap of the density of states, IPT is effective because it facilitates obtaining a real-frequency spectrum in a wide temperature range, including absolute zero.[12] Concerning the effect of U_c in the PAM, several studies have been carried out.[13–17] In Ref. 14, particularly, the authors carried out a systematic analysis of the effect of U_c on the PAM gap using the linearized DMFT. In the present study, we treat the effect of U_c using the perturbative approach to obtain a clear U_c-dependence of the gap, at least in a system weak-coupling regime, and our approach is expected to be complementary to that of Ref. 14.

2. Model and Formulation

We consider the PAM with the Coulomb interaction between the conduction electrons. The Hamiltonian of the current system is defined by

$$\left\{\begin{array}{lcl} \mathcal{H} & \equiv & H - \mu N_{\mathrm{e}}, \\ H & \equiv & \sum\limits_{\boldsymbol{k},\sigma} \varepsilon_{\boldsymbol{k}} c^{\dagger}_{\boldsymbol{k}\sigma} c_{\boldsymbol{k}\sigma} + \varepsilon_f \sum\limits_{i,\sigma} f^{\dagger}_{i\sigma} f_{i\sigma} + V \sum\limits_{i,\sigma} (c^{\dagger}_{i\sigma} f_{i\sigma} + \mathrm{H.c.}) \\ & & + U_f \sum\limits_{i} f^{\dagger}_{i\uparrow} f_{i\uparrow} f^{\dagger}_{i\downarrow} f_{i\downarrow} + U_c \sum\limits_{i} c^{\dagger}_{i\uparrow} c_{i\uparrow} c^{\dagger}_{i\downarrow} c_{i\downarrow}, \\ N_{\mathrm{e}} & \equiv & \sum\limits_{i,\sigma} (c^{\dagger}_{i\sigma} c_{i\sigma} + f^{\dagger}_{i\sigma} f_{i\sigma}), \end{array}\right. \tag{1}$$

where μ denotes the chemical potential. Annihilation (creation) operators of conduction and f electrons with a spin σ on the i-th site are denoted by $c^{(\dagger)}_{i\sigma}$ and $f^{(\dagger)}_{i\sigma}$, respectively. For the conduction-electron operator, $c^{(\dagger)}_{\boldsymbol{k}\sigma}$ is the Fourier transformation of $c^{(\dagger)}_{i\sigma}$. The kinetic energy of a conduction electron and the energy level of an f electron are denoted by $\varepsilon_{\boldsymbol{k}}$ and ε_f, respectively. The hybridization matrix element between f and the conduction electrons is assumed to be local and real, and it is denoted by V. The fourth and fifth terms of H in Eq. (1) are the on-site Coulomb interaction energies between the f electrons and the conduction electrons, respectively.

In the PAM, a conduction electron hybridizes with an f electron and forms a hybridization band. Under the condition of the particle-hole symmetry in the PAM with a non-dispersive f-electron energy level, the band has a hybridization gap at the Fermi level and the ground state of the system is insulating for the non-interacting case: $U_f = 0$. Even for the interacting case, the ground state of the system under the particle-hole symmetric condition remains guaranteed to be insulated with the renormalized hybridization gap because of the Luttinger's theorem .[18] Thus, the conventional PAM with the particle-hole symmetry has been used as the theoretical model of the Kondo insulator / semiconductor. [4,5] In the present system, described by the above Hamiltonian Eq. (1) under the particle-hole symmetric condition expressed as

$$\varepsilon_f + \frac{U_f}{2} = \frac{U_c}{2} = \mu, \tag{2}$$

the Luttinger's theorem also ensures that the Fermi level is always in the renormalized hybridization gap at the absolute zero. Therefore, the PAM with U_c under the condition Eq. (2) is suitable to investigate the effects of U_c on the renormalized hybridization gap.

We apply the DMFT to the present model described by Eq. (1) with a local approximation for the self energy of the Green ' s function. To investigate the correlation effect on the renormalized hybridization gap, an excitation gap clearly defined at the absolute zero is required. For the calculation in a wide temperature range, including the absolute zero, we use the IPT as the DMFT impurity solver as mentioned in Sect. 1. It is known that IPT is effective for the single-band Hubbard model with the particle-hole symmetry since the second-order self energy obtained by the IPT becomes exact in the atomic limit.[10] As shown below, it is expected that IPT is also effective for the PAM with U_c under the particle-hole symmetric condition. Under the particle-hole symmetric condition Eq. (2), Green's function matrix is expressed as

$$\begin{pmatrix} G_{cc\boldsymbol{k}}(z) & G_{cf\boldsymbol{k}}(z) \\ G_{fc\boldsymbol{k}}(z) & G_{ff\boldsymbol{k}}(z) \end{pmatrix} = \begin{pmatrix} z - \varepsilon_{\boldsymbol{k}} - \tilde{\Sigma}_{cc}(z) & -V - \Sigma_{cf}(z) \\ -V - \Sigma_{fc}(z) & z - \tilde{\Sigma}_{ff}(z) \end{pmatrix}^{-1}, \tag{3}$$

where $\tilde{\Sigma}_{\lambda\lambda}(z)$ ($\lambda = c, f$) denotes the diagonal element of the self-energy matrix without the Hartree term and the off-diagonal element of the self-energy matrix is denoted by $\Sigma_{cf}(z)$ (which is equal to $\Sigma_{fc}(z)$). In Eq. (3), the spin index is omitted, as we consider only the paramagnetic state.

With the local approximation, self-energy becomes $\boldsymbol{k}$-independent, and the $\boldsymbol{k}$-dependence of Green's function is expressed only through $\varepsilon_{\boldsymbol{k}}$. Thus, we can express Green's function as

$$G_{\lambda\lambda'}(z; \varepsilon_{\boldsymbol{k}}) \equiv G_{\lambda\lambda'\boldsymbol{k}}(z) \quad (\lambda, \lambda' = c, f). \tag{4}$$

Consequently, the $\boldsymbol{k}$-summation is also replaced by the energy integral with the density of states (DOS) for the unperturbed (non-interacting) system $\rho_0(\nu)$ defined by

$$\rho_0(\nu) \equiv \frac{1}{N}\sum_{\boldsymbol{k}} \delta(\nu - \varepsilon_{\boldsymbol{k}}). \tag{5}$$

Hereafter, $\rho_0(\nu)$ is referred to as free DOS. In Eq. (5), N denotes a number of $\boldsymbol{k}$-points in the first Brillouin zone.

The local approximation of the self energy becomes exact in the infinite-dimensional limit, and it is well-known that the DOS of the tight-binding model with nearest-neighbor hoppings in the hypercubic lattice in infinite dimensions has the Gaussian shape.[19] In the system with the Gaussian DOS, strictly speaking, the hybridization gap does not open because there are *no* band edges in the Gaussian DOS. To consider a well-defined hybridization gap, we use a semi-elliptic form for the free DOS with clearly defined band edges. The semi-elliptic form is known as the DOS for the Bethe lattice with infinite connectivity.[20] In the present calculation, we define the semi-elliptic free DOS as

$$\rho_0(\nu) = \begin{cases} \dfrac{2}{\pi D}\sqrt{1-\left(\dfrac{\nu}{D}\right)^2} & (|\nu| \le D) \\ 0 & (|\nu| > D) \end{cases}, \tag{6}$$

where the half band width is denoted by D.

The hybridization gap is defined by the energy difference between the bottom of the upper hybridization band and the top of the lower hybridization band. Under the particle-hole symmetric condition Eq. (2), the energy dispersion, denoted by $E_0^{\pm}(\varepsilon_{\boldsymbol{k}})$ of the hybridization band of the non-interacting system, is expressed as

$$E_0^{\pm}(\varepsilon_{\boldsymbol{k}}) = \frac{1}{2}\left(\varepsilon_{\boldsymbol{k}} \pm \sqrt{\varepsilon_{\boldsymbol{k}}^2 + 4V^2}\right). \tag{7}$$

Subsequently, the hybridization gap Δ_0 of the non-interacting system is obtained as follows

$$\Delta_0 \equiv E_0^{+}(-D) - E_0^{-}(D) = \sqrt{D^2 + 4V^2} - D. \tag{8}$$

By using the free DOS $\rho_0(\nu)$, the local Green's function matrix is expressed as

$$\hat{G}(z) \equiv \begin{pmatrix} G_{cc}(z) & G_{cf}(z) \\ G_{fc}(z) & G_{ff}(z) \end{pmatrix} = \int d\nu \rho_0(\nu) \begin{pmatrix} G_{cc}(z;\nu) & G_{cf}(z;\nu) \\ G_{fc}(z;\nu) & G_{ff}(z;\nu) \end{pmatrix}. \tag{9}$$

In the DMFT, the local Green's function is also expressed by introducing the Weiss function (or the cavity Green's function) as

$$\hat{G}^{-1}(z) = \hat{\mathcal{G}}^{-1}(z) - \hat{\Sigma}(z), \tag{10}$$

where the Weiss-function matrix $\hat{\mathscr{G}}(z)$ and the self-energy matrix $\hat{\Sigma}(z)$ are defined by

$$\hat{\mathscr{G}}(z) \equiv \begin{pmatrix} \tilde{\mathscr{G}}_{cc}(z) & \mathscr{G}_{cf}(z) \\ \mathscr{G}_{fc}(z) & \tilde{\mathscr{G}}_{ff}(z) \end{pmatrix}, \tag{11}$$

$$\hat{\Sigma}(z) \equiv \begin{pmatrix} \tilde{\Sigma}_{cc}(z) & \Sigma_{cf}(z) \\ \Sigma_{fc}(z) & \tilde{\Sigma}_{ff}(z) \end{pmatrix}. \tag{12}$$

In the expression of the Weiss-function matrix Eq. (11), $\tilde{\mathscr{G}}_{\lambda\lambda}(z)$ denotes the Weiss function in which the Hartree term of the self energy is subtracted from $\mathscr{G}_{\lambda\lambda}(z)$ ($\lambda = c, f$).

In the IPT scheme, the self energy is approximated by the second-order perturbative contribution composed of the Weiss functions as

$$\Sigma_{\lambda\lambda'}(z) \simeq -U_\lambda U_{\lambda'} T \sum_l T \sum_m \mathscr{G}_{\lambda\lambda'}(i\varepsilon_l)\mathscr{G}_{\lambda\lambda'}(i\varepsilon_m)\mathscr{G}_{\lambda\lambda'}(z - i\varepsilon_l + i\varepsilon_m) \quad (\lambda, \lambda' = c, f), \tag{13}$$

where T denotes the temperature of the system, and ε_l and ε_m are fermionic Matsubara frequencies. In Eq. (13), the tilde marks in the notations of the diagonal elements of the Weiss-function matrix and the self-energy matrix have been omitted for simplicity. Using the spectral representation, the right side of Eq. (13) is also expressed as

$$U_\lambda U_{\lambda'} \iiint d\varepsilon_1 d\varepsilon_2 d\varepsilon_3 \varrho_{\lambda\lambda'}(\varepsilon_1)\varrho_{\lambda\lambda'}(\varepsilon_2)\varrho_{\lambda\lambda'}(\varepsilon_3)\frac{f(\varepsilon_1)f(-\varepsilon_2)f(\varepsilon_3) + f(-\varepsilon_1)f(\varepsilon_2)f(-\varepsilon_3)}{z - \varepsilon_1 + \varepsilon_2 - \varepsilon_3}, \tag{14}$$

where $\varrho_{\lambda\lambda'}(\varepsilon)$ is defined by the imaginary part of the Weiss function as

$$\varrho_{\lambda\lambda'}(\varepsilon) \equiv -\frac{1}{\pi}\mathrm{Im}\mathscr{G}_{\lambda\lambda'}(\varepsilon + i\eta) \quad (\lambda, \lambda' = c, f), \tag{15}$$

with a positive infinitesimal η. In Eq. (14), $f(\varepsilon)$ is the Fermi distribution function defined as $f(\varepsilon) \equiv 1/(e^{\varepsilon/T} + 1)$. By self-consistently solving Eqs. (3), (9), (10) , and (14), we can obtain f-electron local DOS $\rho_f(\varepsilon)$ and conduction-electron local DOS $\rho_c(\varepsilon)$ defined as

$$\rho_f(\varepsilon) \equiv -\frac{1}{\pi}\,\mathrm{Im}\,G_{ff}(\varepsilon + i\eta), \tag{16}$$

$$\rho_c(\varepsilon) \equiv -\frac{1}{\pi}\,\mathrm{Im}\,G_{cc}(\varepsilon + i\eta). \tag{17}$$

Here, let us comment on the reason why it is valid that the IPT is also effective for the PAM with U_c under the particle-hole symmetric condition. In the usual PAM without U_c under the particle-hole symmetric condition, the f-component $G_{ff}(i\varepsilon_n)$ of the local Green's function matrix in the atomic limit $U_f/V \to \infty$ is expressed as

$$G_{ff}(i\varepsilon_n) = \frac{1}{2}\left(\frac{1}{i\varepsilon_n - \varepsilon_f} + \frac{1}{i\varepsilon_n - (\varepsilon_f + U_f)}\right)$$

$$= \frac{1}{2}\left(\frac{1}{i\varepsilon_n + \frac{U_f}{2}} + \frac{1}{i\varepsilon_n - \frac{U_f}{2}}\right)$$

$$= \left(i\varepsilon_n - \frac{U_f^2}{4i\varepsilon_n}\right)^{-1}. \tag{18}$$

In the IPT, the self energy without the Hartree term is obtained similarly to the case in the single-band Hubbard model[10) as

$$\tilde{\Sigma}_{ff}(i\varepsilon_n) = \frac{U_f^2}{4i\varepsilon_n}, \tag{19}$$

with setting in Eqs. (13) and (14) as

$$\tilde{\mathcal{G}}_{ff}(i\varepsilon_n) = 1/(i\varepsilon_n). \tag{20}$$

Since $G_{ff}(i\varepsilon_n)$ is expressed as $(G_{ff}(i\varepsilon_n))^{-1} = (\tilde{\mathcal{G}}_{ff}(i\varepsilon_n))^{-1} - \tilde{\Sigma}_{ff}(i\varepsilon_n)$ in the DMFT scheme, Eqs. (18), (19), and (20) show that the Weiss function and the self energy in the IPT can consistently construct the exact local Green's function of the PAM in the atomic limit with the particle-hole symmetry. Thus, it is also expected that the IPT is effective for the PAM with U_c under the particle-hole symmetric condition as long as we focus on the weak-coupling regime for U_c smaller than U_f in the present study.

3. Results

In the present calculation, we take the half band width D in the free DOS Eq. (6) as the energy unit: $D = 1$. The hybridization energy V is set to 0.5 in the numerical results shown below.

First, we show the U_f-dependences of $\rho_f(\varepsilon)$ (Fig. 1) and $\rho_c(\varepsilon)$ (Fig. 2) for $U_c = 0$ at the absolute zero. The hybridization gap opens at the Fermi level ($\varepsilon = 0$) and narrows with the increase of U_f. The narrowing of the hybridization gap reflects the renormalization effect of U_f. As the enhancement of the correlation effect with the increase of U_f corresponds to the relative suppression of the effective hybridization energy, the form of the conduction-electron DOS near the Fermi level approaches that of the original free DOS Eq. (6) with an increase in U_f, as shown in Fig. 2. Sharp peaks are found to appear at high energy for higher U_f values. These peaks correspond to the lower and upper Hubbard bands.

Figure 3 shows the U_c-dependence of $\rho_f(\varepsilon)$ for $U_f = 2.0$ at the absolute zero. It can be seen that the hybridization gap widens as U_c increases. As U_c is smaller than U_f in the present case, only the low-energy structure of the spectrum, including the hybridization gap, is affected by U_c. This trend is much clearer in the spectrum for $U_f = 5.0$, as shown in Fig. 4.

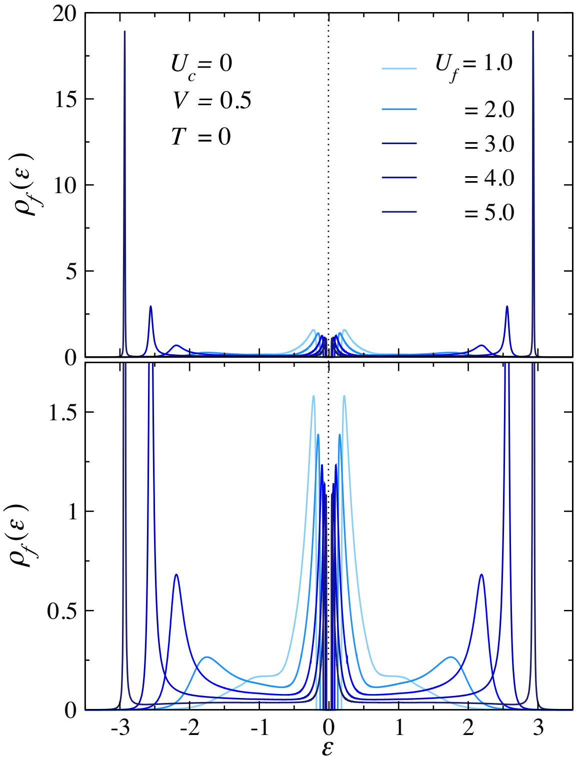

Fig. 1. (Color online) Spectra of the f-electron local DOS $\rho_f(\varepsilon)$ at $T = 0$ for $U_c = 0$ and several U_f values. The lower panel shows the enlarged DOS figure.

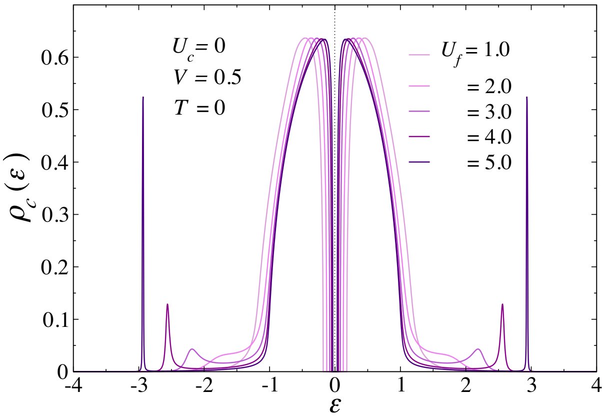

Fig. 2. (Color online) Spectra of the conduction-electron local DOS $\rho_c(\varepsilon)$ at $T = 0$ for $U_c = 0$ and several U_f values.

To quantitatively investigate the correlation effect by U_c on the spectrum at the absolute zero, we estimate the renormalized hybridization gap of the quasiparticle band. In the quasiparticle picture, the energy dispersion of the renormalized hybridization band is expressed

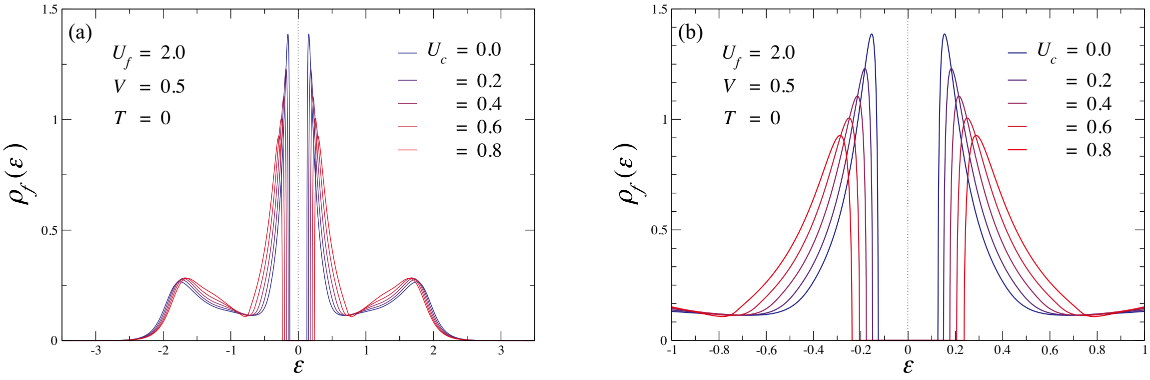

Fig. 3. (Color online) (a) Spectra of the f-electron local DOS $\rho_f(\varepsilon)$ at $T = 0$ for $U_f = 2.0$ and several U_c values. (b) Enlarged DOS figure near the Fermi level.

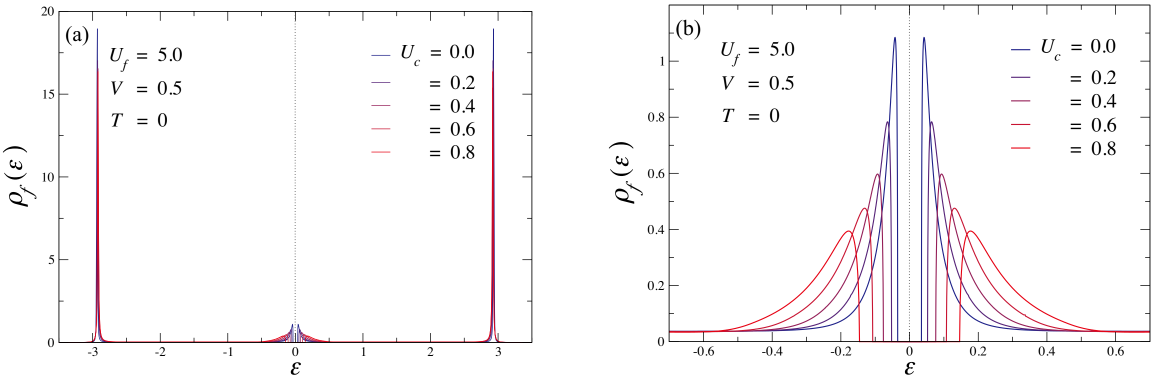

Fig. 4. (Color online) (a) Spectra of the f-electron local DOS $\rho_f(\varepsilon)$ at $T = 0$ for $U_f = 5.0$ and several U_c values. (b) Enlarged DOS figure near the Fermi level.

as

$$E^{\pm}(\varepsilon_{\boldsymbol{k}}) = \frac{1}{2}\left(z_c\varepsilon_{\boldsymbol{k}} \pm \sqrt{(z_c\varepsilon_{\boldsymbol{k}})^2 + 4\tilde{V}^2}\right), \tag{21}$$

where renormalization factors z_c and z_f, and the effective hybridization energy (EHE) $\tilde{V}$ are defined by

$$z_c \equiv \left(1 - \frac{d\,\mathrm{Re}\,\Sigma_{cc}(\varepsilon + i\eta)}{d\varepsilon}\bigg|_{\varepsilon=0}\right)^{-1}, \tag{22}$$

$$z_f \equiv \left(1 - \frac{d\,\mathrm{Re}\,\Sigma_{ff}(\varepsilon + i\eta)}{d\varepsilon}\bigg|_{\varepsilon=0}\right)^{-1}, \tag{23}$$

$$\tilde{V} \equiv \sqrt{z_c z_f}\,V^*, \tag{24}$$

$$V^* \equiv V + \mathrm{Re}\,\Sigma_{cf}(\varepsilon + i\eta)\big|_{\varepsilon=0} = V + \mathrm{Re}\,\Sigma_{cf}(i\eta). \tag{25}$$

The renormalized hybridization gap denoted by $\Delta_{\rm QP}$ for the quasiparticle is defined as $\Delta_{\rm QP} \equiv E^{+}(-D) - E^{-}(D)$. We introduce the renormalized band width defined by

$$\tilde{D} \equiv z_c D, \tag{26}$$

to obtain the $\Delta_{\rm QP}$ expression as

$$\Delta_{\rm QP} = \sqrt{\tilde{D}^2 + 4\tilde{V}^2} - \tilde{D}, \tag{27}$$

which is similar to Eq. (8).

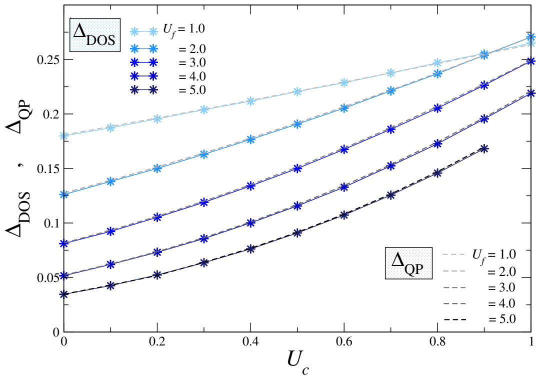

Fig. 5. (Color online) U_c-dependence of $\Delta_{\rm DOS}$ and $\Delta_{\rm QP}$ for several U_f values.

As the renormalization factor and the EHE are obtained from the numerical results of the self energies by Eqs. (22)-(25), we can estimate the renormalized hybridization gap $\Delta_{\rm QP}$ in the quasiparticle picture with the use of Eq. (27). On the other hand, the hybridization gap can be directly obtained from the local DOS spectrum $\rho_f(\varepsilon)$ (or $\rho_c(\varepsilon)$). Here, we define the DOS gap, denoted by $\Delta_{\rm DOS}$, as the energy region in which $\rho_f(\varepsilon)$ has numerically the zero value around the Fermi level at $T = 0$. If the value of $\Delta_{\rm QP}$, defined by Eq. (27), is consistent with that of $\Delta_{\rm DOS}$, the quasiparticulate picture of the system can be expected to be valid. Figure 5 shows the U_c-dependence of the DOS gap $\Delta_{\rm DOS}$ and the renormalized hybridization gap $\Delta_{\rm QP}$ defined by Eq. (27). It can be seen that the U_c-dependence of $\Delta_{\rm DOS}$ is well approximated by that of $\Delta_{\rm QP}$ for all the investigated U_f values. Thus, we can conclude that it is valid to describe the system by the quasiparticle picture in the energy region around the hybridization gap. Although the DOS gap is narrowed by the renormalization effect of U_f, it increases with the increase of U_c for all U_f values.

U_c-dependences of enhancement factors z_f^{-1} and z_c^{-1} are shown in Fig. 6. The larger that

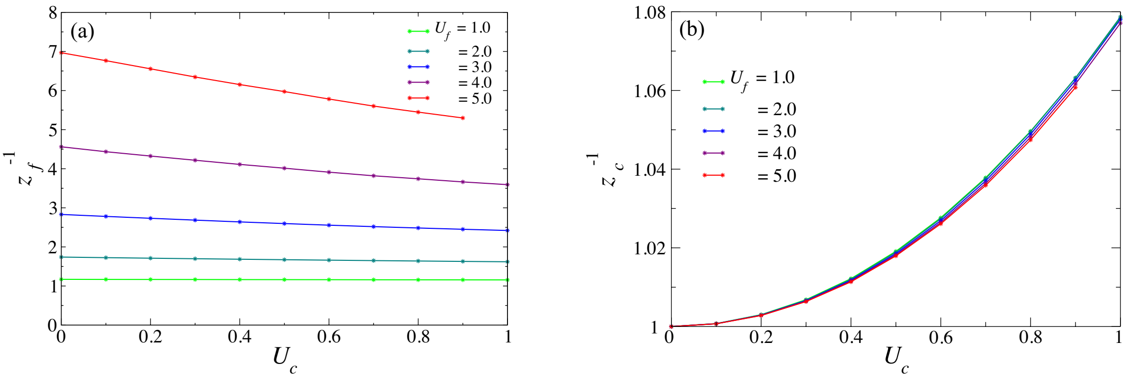

Fig. 6. (Color online) U_c-dependence of enhancement factors (a) z_f^{-1} and (b) z_c^{-1} for $U_f = 1.0$ at $T = 0$.

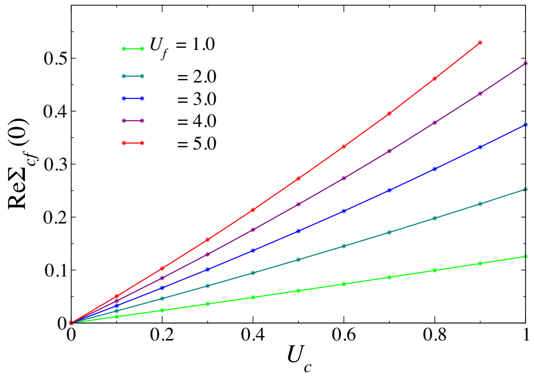

Fig. 7. (Color online) U_c-dependence of $\mathrm{Re}\Sigma_{cf}(i\eta)$ for $U_f = 1.0$ at $T = 0$.

U_f becomes, the more that the enhancement factor z_f^{-1} is suppressed with increasing U_c, as shown in Fig. 6(a). The enhancement factor z_c^{-1} shows a quadratic growth of U_c from $z_c^{-1} = 1$ for any value of U_f reflecting the second-order contribution of the self energy Eq. (14). In Fig. 7, we show the U_c-dependence of the real part ($\mathrm{Re}\,\Sigma_{cf}(i\eta)$) of the c-f element of the self-energy matrix at $\varepsilon = 0$. For small U_c values, $\mathrm{Re}\,\Sigma_{cf}(i\eta)$ increases linearly with the increase of U_c, as expected from Eq. (14).

Let us estimate the renormalized hybridization gap Δ_{QP} defined by Eq. (27) by the perturbative approach. The renormalization factors z_f and z_c are expressed as $z_f = 1 + O\left(U_f^2\right)$ and $z_c = 1 + O\left(U_c^2\right)$ based on Eqs. (22) and (23), respectively. The enhanced hybridization energy V^* can be expressed up to the lowest order of U_c and U_f as

$$V^* = V + \alpha_{cf} U_f U_c + O\left(U_f^2\right) + O\left(U_c^2\right), \tag{28}$$

where α_{cf} is a constant independent from U_f and U_c. Eqs. (A·10) and (A·11) in the Appendix ensure that α_{cf} is positive at least in the weak-coupling regime.

Substitute Eq. (28) in Eq. (24) to obtain

$$\tilde{V} = \sqrt{z_c z_f} V^* = V + \alpha_{cf} U_c U_f + \mathcal{O}\left(U_f^2\right) + \mathcal{O}\left(U_f^2\right). \tag{29}$$

Using Eq. (29) and considering that $\tilde{D} = D + \mathcal{O}\left(U_c^2\right)$, by Eq. (26), we can estimate Δ_{QP} from Eq. (27) ignoring $\mathcal{O}\left(U_c^2\right)$ and $\mathcal{O}\left(U_f^2\right)$ as follows;

$$\begin{aligned} \Delta_{\mathrm{QP}} &\simeq \sqrt{D^2 + 4(V + \alpha_{cf} U_c U_f)^2} - D \\ &\simeq \Delta_0 + \frac{4\alpha_{cf} V}{\sqrt{D^2 + 4V^2}} U_c U_f, \end{aligned} \tag{30}$$

where the unperturbed hybridization gap Δ_0 is defined by Eq. (8). Is is clear from Eq. (30) that the effective hybridization gap Δ_{QP} is *enhanced* by U_c because of the positivity of α_{cf} to the system with a fixed value of U_f.

The finite temperature system results are shown below. For the conventional PAM without U_c, hybridization between conduction and f electrons is expected to be effectively weakened at a higher temperature than EHE.[12] We call this situation the c-f separation hereafter.[12] In Figs. 8 and 9, temperature dependences of $\rho_f(\varepsilon)$ and $\rho_c(\varepsilon)$ of the system without U_c for $U_f = 2.0$ are shown, respectively. As expected, the hybridization gap fills as the temperature increases and the gap structure disappears completely at much higher temperatures than $\tilde{V}$. The spectrum of $\rho_f(\varepsilon)$ at high temperature has two peaks near $\varepsilon \simeq \pm U_f/2$ corresponding to the upper and lower Hubbard bands. In contrast, the spectrum of $\rho_c(\varepsilon)$ at high temperature has a similar form to the free DOS $\rho_0(\varepsilon)$, which is the DOS whose system consists only of conduction electrons. These results reflect the c-f separation.

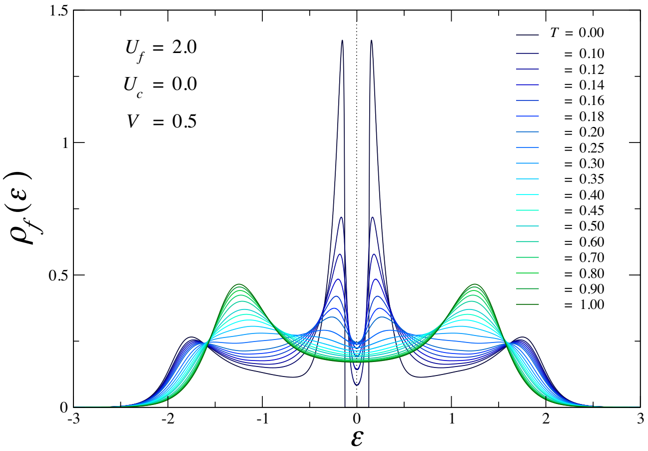

Fig. 8. (Color online) Temperature dependence of $\rho_f(\varepsilon)$ for $U_f = 2.0$ and $U_c = 0.0$.

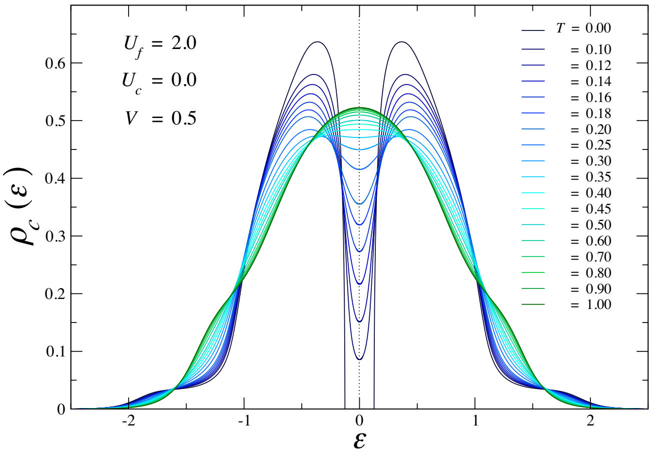

Fig. 9. (Color online) Temperature dependence of $\rho_c(\varepsilon)$ for $U_f = 2.0$ and $U_c = 0.0$.

Figures 10(a)-(c) show the temperature dependences of $\rho_f(\varepsilon)$ and $\rho_c(\varepsilon)$ for $U_f = 2.0$ and various U_c values. Generally, the gap can be seen to be filled with increasing temperatures. As U_c increases, the DOS gap widens, and the temperature at which the gap begins to fill seems to change. In the system with the $\Delta_{\rm DOS}$ gap at the Fermi level, the electron begins to be excited at $T \sim \Delta_{\rm DOS}$ and the electronic state begins to be reconstructed by the correlation effect. Thus, it is natural to consider that the temperature at which the gap begins to be filled corresponds to the DOS gap $\Delta_{\rm DOS}$ itself.

To investigate the correlation effect of U_c on the temperature at which the electronic state begins to be reconstructed, it is necessary to define quantitatively the characteristic temperature that represents the temperature at which the gap begins to be filled. In the present study, the above characteristic temperature is denoted by $T_{\rm gap}^{f(c)}$, and we define $T_{\rm gap}^{f(c)}$ as follows. First, we consider the ratio of the value $\rho_{f(c)}(0)$ of the DOS at $\varepsilon = 0$ (the Fermi level) to the peak value $\rho_{f(c)}(\varepsilon_{\rm peak}^{f(c)})$ of the DOS near the gap, where $\varepsilon_{\rm peak}^{f(c)}$ denotes the energy at which the peak of the DOS $\rho_{f(c)}(\varepsilon)$ exists near the gap, as shown in Fig. 11(a). This ratio $\rho_{f(c)}(0)/\rho_{f(c)}(\varepsilon_{\rm peak}^{f(c)})$ at temperature T is denoted by $R^{f(c)}(T)$. Furthermore, we define the characteristic temperature $T_{\rm gap}^{f(c)}$ as the temperature at which the value of $\rho_{f(c)}(0)$ becomes a ten percent of that of $\rho_{f(c)}(\varepsilon_{\rm peak}^{f(c)})$. Namely, $T_{\rm gap}^{f(c)}$ is defined as the temperature at which the following equation is supported;

$$R^{f(c)}(T_{\rm gap}^{f(c)}) = 0.1, \tag{31}$$

as shown in Fig. 11(b).

We show temperature dependences of $R^f(T)$ and $R^c(T)$ in Figs. 12 and 13, respectively. It is shown that both $R^f(T)$ and $R^c(T)$ increase more slowly with the increase of T for a higher

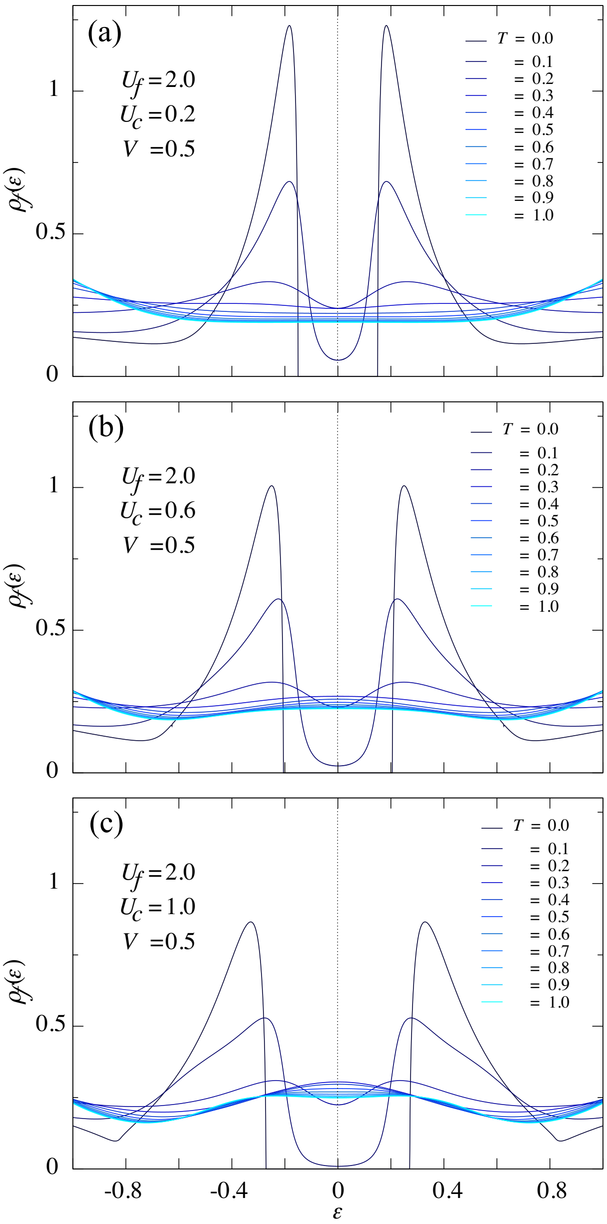

Fig. 10. (Color online) Temperature dependence of $\rho_f(\varepsilon)$ for $U_f = 2.0$ and (a) $U_c = 0.2$, (b) $U_c = 0.6$, and (c) $U_c = 1.0$.

U_c value. The characteristic temperature $T_{\rm gap}^{f(c)}$ is given by the intersection that satisfies Eq. (31). In the numerical estimation of the value of $T_{\rm gap}^{f(c)}$, we regard a curve between $R^{f(c)}(T_n)$ and $R^{f(c)}(T_{n+1})$ as a straight line for the calculated n-th and $(n + 1)$-th points of temperature T_n and T_{n+1} in the determination of these intersections.

To compare the correlation effect of U_c on $T_{\rm gap}^{f(c)}$ to that of $\Delta_{\rm DOS}$, these values are scaled by those for $U_c = 0$. Indicating these values as functions of U_c by $\Delta_{\rm DOS}(U_c)$ and $T_{\rm gap}^{f(c)}(U_c)$,

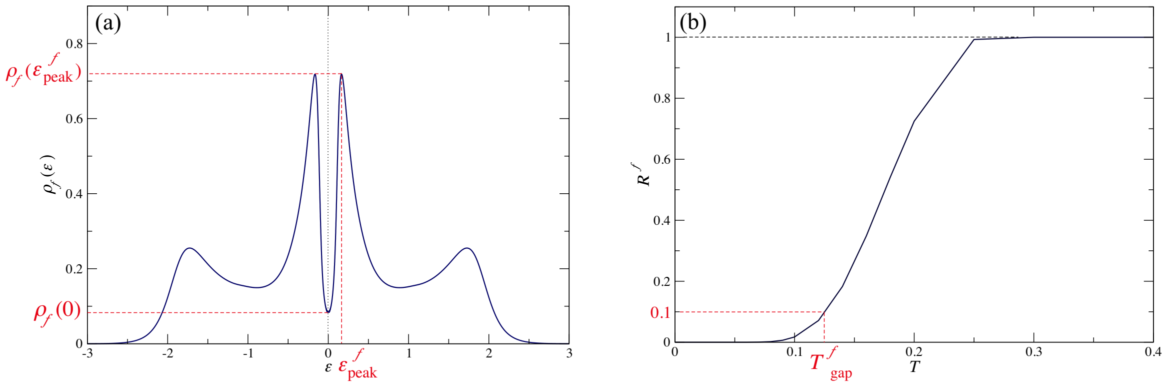

Fig. 11. (Color online) (a) Schematic explanation of the peak energy $\varepsilon^f_{\rm peak}$. The ratio $R^f(T)$ is defined by $R^f(T) = \rho_f(0)/\rho_f(\varepsilon^f_{\rm peak})$. (b) Schematic explanation of the characteristic temperature $T^f_{\rm gap}$.

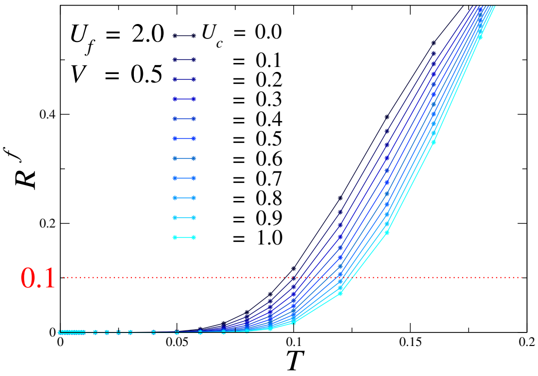

Fig. 12. (Color online) Temperature dependence of $R^f(T)$ for $U_f = 2.0$ and several U_c values.

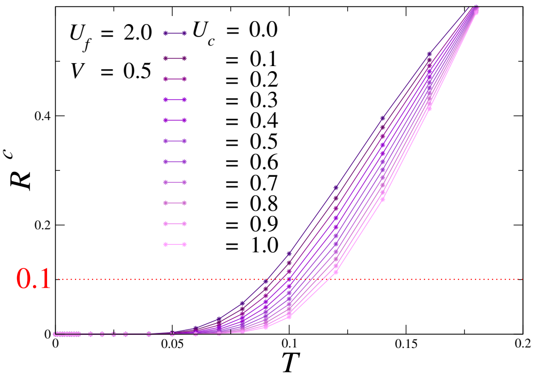

Fig. 13. (Color online) Temperature dependence of $R^c(T)$ for $U_f = 2.0$ and several U_c values.

we define scaled quantities $\delta_{\rm DOS}$ and $t_{\rm gap}^{f(c)}$ as

$$\delta_{\rm DOS} \equiv \frac{\Delta_{\rm DOS}(U_c)}{\Delta_{\rm DOS}(0)}, \tag{32}$$

$$t_{\rm gap}^{f(c)} \equiv \frac{T_{\rm gap}^{f(c)}(U_c)}{T_{\rm gap}^{f(c)}(0)}. \tag{33}$$

Figure 14 shows U_c-dependences of $t_{\rm gap}^{f}$, $t_{\rm gap}^{c}$, and $\delta_{\rm DOS}$. Evidently, U_c-dependences of $t_{\rm gap}^{f}$, and $t_{\rm gap}^{c}$ are very similar. Moreover, it should be emphasized that both $t_{\rm gap}^{f(c)}$ and $\delta_{\rm DOS}$ are monotonously increasing functions of U_c in the region we have calculated.

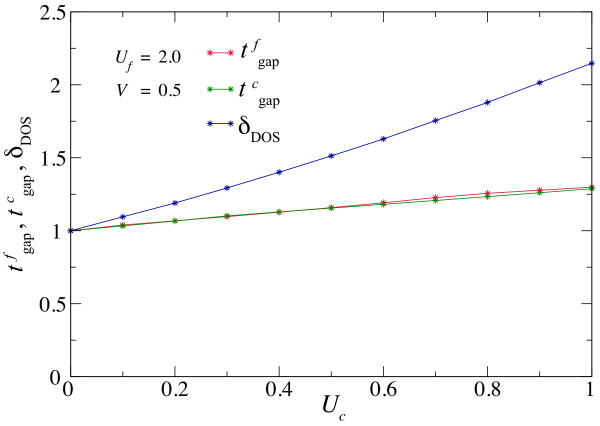

Fig. 14. (Color online) U_c-dependences of $t_{\rm gap}^{f}$, $t_{\rm gap}^{c}$, and $\delta_{\rm DOS}$ for $U_f = 2.0$.

4. Summary and Discussion

In summary, we have treated the theoretical model of the Kondo insulator based on the PAM with the Coulomb interaction energy U_c between conduction electrons by the DMFT in which the IPT is used as the impurity solver. We have investigated U_c-dependence of the hybridization gap and temperature dependence of the density of states.

It is well-known that the hybridization gap in the usual PAM narrows because of the renormalization effect by the Coulomb interaction energy U_f between the f electrons. In this study, it has been shown that the hybridization gap for the system with a fixed U_f value is widened by U_c. The DOS gap (the gap of the density of states) at absolute zero can be considered as the renormalized hybridization gap, and the DOS gap can be expressed using the renormalization factor. Actually, we have confirmed that the DOS gap $\Delta_{\rm DOS}$ obtained by numerical calculation is quantitatively consistent with the renormalized hybridization gap $\Delta_{\rm QP}$ that is expressed by the renormalization factor defined by the self energy. Therefore, we can conclude that it is valid to analyze the interaction-energy dependence of the DOS gap using the renormalization factor. This U_c-dependence of the DOS gap at the absolute zero is qualitatively consistent with the result obtained by the linearized DMFT in Ref.14.

Although the DOS gap at the absolute zero can be estimated by the renormalization factor, the correlation effect that is reflected in the temperature dependence of the DOS is not trivial. The temperature at which the electronic state begins to be reconstructed and the DOS begins to show temperature dependence is expected to be $T \sim \Delta_{\rm DOS}$. In the present study, we have defined $T_{\rm gap}^{f(c)}$ in Eq. (31) as the abovementioned temperature. In addition, U_c-dependence of $T_{\rm gap}^{f(c)}$ was investigated. Additionally, it has been shown that $T_{\rm gap}^{f(c)}$ also increases as U_c increases similarly to the U_c-dependence of the DOS gap.

As mentioned in Sec.1, Itai and Fazekas reported that the hybridization gap in the PAM with infinite U_f and finite U_c narrows as U_c increases.[9] However, Shibata et al. showed that the excitation gap of the KLM with finite U_c is widened by U_c.[8] In Ref.9, a bare V-value of the hybridization energy appears in EHE $\tilde{V}$ as $\tilde{V} = \sqrt{z_f z_c} V$. According to our analysis, however, the hybridization energy contributing to $\tilde{V}$ is not the bare V but V^* defined by Eq. (25), which involves the real part of the c-f component of the self energy as $\tilde{V} = \sqrt{z_f z_c} V^* = \sqrt{z_f z_c}\left(V + {\rm Re}\,\Sigma_{cf}(i\eta)\right)$.

In the EHE expression $\tilde{V} = \sqrt{z_f z_c} V$ given by Itai and Fazekas, EHE decreases monotonically with the increase of U_c as this expression involves only z_c, which is simply suppressed by U_c. In Eq. (29) obtained by the present study, however, it has been found that the enhancement of V^* is stronger than the suppression of z_c with the increase of U_c, at least in the weak-coupling regime, owing to the existence of the U_c-linear term in ${\rm Re}\,\Sigma_{cf}^{(2)}(i\eta)$. Thus, it is concluded that the hybridization gap in the theoretical model of the Kondo insulator is widened by U_c, at least in the weak-coupling regime.

Acknowledgments

A part of numerical calculations in this work has been done using the supercomputer of ACCMS, Kyoto University.

Appendix

This Appendix derives the effective hybridization energy in a lower-energy region based on the perturbative treatment of the self energy. We consider the second-order contribution $\Sigma_{cf}^{(2)}(i\varepsilon_n)$ of the c-f component of the self-energy matrix under the particle-hole symmetric condition. The c-f component $G_{cf}^{(0)}(i\varepsilon_n)$ of the local Green's function matrix of the unperturbed system has the spectral representation as

$$G_{cf}^{(0)}(i\varepsilon_n) = \int_{-\infty}^{\infty} d\varepsilon \frac{\rho_{cf}^{(0)}(\varepsilon)}{i\varepsilon_n - \varepsilon}, \tag{A·1}$$

where

$$\rho_{cf}^{(0)}(\varepsilon) = -\frac{1}{\pi} \operatorname{Im} G_{cf}^{(0)}(\varepsilon + i\eta).$$

Therefore, the second-order contribution $\Sigma_{cf}^{(2)}(i\varepsilon_n)$ to the c-f component of the self-energy matrix under the particle-hole symmetric condition is expressed as follows:

$$\begin{aligned} \Sigma_{cf}^{(2)}(i\varepsilon_n) &= -U_c U_f T \sum_l T \sum_m G_{cf}^{(0)}(i\varepsilon_l) G_{cf}^{(0)}(i\varepsilon_m) G_{cf}^{(0)}(i\varepsilon_n - i\varepsilon_l + i\varepsilon_m) \\ &= U_c U_f \iiint d\varepsilon_1 d\varepsilon_2 d\varepsilon_3 \rho_{cf}^{(0)}(\varepsilon_1) \rho_{cf}^{(0)}(\varepsilon_2) \rho_{cf}^{(0)}(\varepsilon_3) \frac{f(\varepsilon_1) f(\varepsilon_2) f(-\varepsilon_3) + f(-\varepsilon_1) f(-\varepsilon_2) f(\varepsilon_3)}{i\varepsilon_n - \varepsilon_1 - \varepsilon_2 + \varepsilon_3}. \end{aligned} \tag{A·2}$$

With an analytic continuation $i\varepsilon_n \to \varepsilon + i\eta$, the imaginary part $\operatorname{Im} \Sigma_{cf}^{(2)}(\varepsilon + i\eta)$ of the self energy Eq. (A·2) is expressed as

$$\begin{aligned} \operatorname{Im} \Sigma_{cf}^{(2)}(\varepsilon + i\eta) = -\pi U_c U_f &\iiint d\varepsilon_1 d\varepsilon_2 d\varepsilon_3 \rho_{cf}^{(0)}(\varepsilon_1) \rho_{cf}^{(0)}(\varepsilon_2) \rho_{cf}^{(0)}(\varepsilon_3) \\ &\cdot \left[f(\varepsilon_1) f(\varepsilon_2) f(-\varepsilon_3) + f(-\varepsilon_1) f(-\varepsilon_2) f(\varepsilon_3) \right] \delta(\varepsilon - \varepsilon_1 - \varepsilon_2 + \varepsilon_3). \end{aligned} \tag{A·3}$$

Let us estimate the integral in the right side of Eq. (A·3) at the absolute zero. Because the Fermi distribution function $f(\varepsilon)$ is expressed as $f(\varepsilon) = \theta(-\varepsilon)$ by the step function at the absolute zero, we can divide the integral in Eq. (A·3) into two terms as

$$\begin{aligned} &\iiint d\varepsilon_1 d\varepsilon_2 d\varepsilon_3 \rho_{cf}^{(0)}(\varepsilon_1) \rho_{cf}^{(0)}(\varepsilon_2) \rho_{cf}^{(0)}(\varepsilon_3) \left[f(\varepsilon_1) f(\varepsilon_2) f(-\varepsilon_3) + f(-\varepsilon_1) f(-\varepsilon_2) f(\varepsilon_3) \right] \delta(\varepsilon - \varepsilon_1 - \varepsilon_2 + \varepsilon_3) \\ &= \left[\int_{-\infty}^{0} d\varepsilon_1 \int_{-\infty}^{0} d\varepsilon_2 \int_{0}^{\infty} d\varepsilon_3 + \int_{0}^{\infty} d\varepsilon_1 \int_{0}^{\infty} d\varepsilon_2 \int_{-\infty}^{0} d\varepsilon_3 \right] \rho_{cf}^{(0)}(\varepsilon_1) \rho_{cf}^{(0)}(\varepsilon_2) \rho_{cf}^{(0)}(\varepsilon_3) \delta(\varepsilon - \varepsilon_1 - \varepsilon_2 + \varepsilon_3). \end{aligned} \tag{A·4}$$

Here, we consider the sign of the function $\rho_{cf}^{(0)}(\varepsilon)$. By denoting the $\boldsymbol{k}$-dependent Green's function similarly to Eq. (4) , the unperturbed c-f Green's function under the particle-hole symmetric condition is expressed as

$$G_{cf}^{(0)}(i\varepsilon_n; \varepsilon_{\boldsymbol{k}}) = \frac{V}{i\varepsilon_n (i\varepsilon_n - \varepsilon_{\boldsymbol{k}}) - V^2}. \tag{A·5}$$

Then, $\rho_{cf}^{(0)}(\varepsilon)$ is expressed by using the free DOS from Eq. (6) as

$$\rho_{cf}^{(0)}(\varepsilon) = \int d\nu \rho_0(\nu)\left(-\frac{1}{\pi}\,\mathrm{Im}\,G_{cf}^{(0)}(\varepsilon + i\eta;\nu)\right) = \begin{cases} \dfrac{V}{\varepsilon}\rho_0\left(\varepsilon - \dfrac{V^2}{\varepsilon}\right) & \left(\left|\varepsilon - \dfrac{V^2}{\varepsilon}\right| \leq D\right), \\ 0 & \left(\left|\varepsilon - \dfrac{V^2}{\varepsilon}\right| > D\right). \end{cases} \tag{A·6}$$

Therefore, $\rho_{cf}^{(0)}(\varepsilon)$ is an odd function of ε and the sign of $\rho_{cf}^{(0)}(\varepsilon)$ is equal to that of ε itself.

In the first term of the right side of Eq. (A·4), the region limited by the argument of the delta function is $\varepsilon = -[|\varepsilon_1| + |\varepsilon_2| + |\varepsilon_3|] \leq 0$ in the intervals of the integral ($\varepsilon_1 \leq 0, \varepsilon_2 \leq 0, \varepsilon_3 \geq 0$). Thus, it holds that $\rho_{cf}^{(0)}(\varepsilon_1) \leq 0, \rho_{cf}^{(0)}(\varepsilon_2) \leq 0, \rho_{cf}^{(0)}(\varepsilon_3) \geq 0$ in these intervals of the integral, as the sign of $\rho_{cf}^{(0)}(\varepsilon)$ is equal to that of ε. Therefore, the first term of the right side of Eq. (A·4) is positive if $\varepsilon < 0$ and is equal to 0 if $\varepsilon \geq 0$.

On the other hand, in the second term of the right side of Eq. (A·4), the region limited by the delta function argument is $\varepsilon = |\varepsilon_1| + |\varepsilon_2| + |\varepsilon_3| \geq 0$ in the intervals of the integral ($\varepsilon_1 \geq 0, \varepsilon_2 \geq 0, \varepsilon_3 \leq 0$), and it holds that $\rho_{cf}^{(0)}(\varepsilon_1) \geq 0, \rho_{cf}^{(0)}(\varepsilon_2) \geq 0, \rho_{cf}^{(0)}(\varepsilon_3) \leq 0$. Thus, the second term of the right side of Eq. (A·4) is negative if $\varepsilon > 0$ and is equal to 0 if $\varepsilon \leq 0$. As it is deduced from these arguments that the sign of the integral in Eq. (A·3) at the absolute zero is opposite to that of ε, we can conclude that

$$\mathrm{sgn}\left(\mathrm{Im}\,\Sigma_{cf}^{(2)}(\varepsilon + i\eta)\right) = \mathrm{sgn}(\varepsilon). \tag{A·7}$$

The real part $\mathrm{Re}\,\Sigma_{cf}^{(2)}(\varepsilon + i\eta)$ of the self-energy is expressed by the Kramars-Kronig (Hilbert) transformation of $\mathrm{Im}\,\Sigma_{cf}^{(2)}(\varepsilon + i\eta)$ as

$$\mathrm{Re}\,\Sigma_{cf}^{(2)}(\varepsilon + i\eta) = \frac{1}{\pi}\mathcal{P}\int_{-\infty}^{\infty} \mathrm{d}\varepsilon'\, \frac{\mathrm{Im}\,\Sigma_{cf}^{(2)}(\varepsilon' + i\eta)}{\varepsilon' - \varepsilon}, \tag{A·8}$$

where $\mathcal{P}$ denotes the Cauchy principal value of the integral. Additionally, we obtain the value $\mathrm{Re}\,\Sigma_{cf}^{(2)}(i\eta)$ at the Fermi level ($\varepsilon = 0$) in Eqs. (24) and (25) as follows:

$$\mathrm{Re}\,\Sigma_{cf}^{(2)}(i\eta) = \frac{1}{\pi}\mathcal{P}\int_{-\infty}^{\infty} \mathrm{d}\varepsilon'\, \frac{\mathrm{Im}\,\Sigma_{cf}^{(2)}(\varepsilon' + i\eta)}{\varepsilon'}. \tag{A·9}$$

As Eq. (A·7) is maintained in the integrand of the right side of Eq. (A·9), we can obtain the relation as

$$\mathrm{Re}\,\Sigma_{cf}^{(2)}(i\eta) \geq 0. \tag{A·10}$$

Therefore, it is found in Eq. (25) that the following relation is always maintained in the weak-coupling region in the sense of the perturbative treatment;

$$V^* \geq V. \tag{A·11}$$

References

1) G. Aeppli and Z. Fisk, Comments Condens. Matter Phys. **16**, 155 (1992).

2) P. Riseborough, Adv. Phys. **49**, 257 (2000).

3) For a review, see, e.g., A. C. Hewson, *The Kondo Problem to Heavy Fermions* (Cambridge University Press, Cambridge, 1997).

4) M. Jarrel, H. Akhlaghpour, and Th. Pruschke, Phys. Rev. Lett. **70**, 1670 (1993); M. Jarrel, Phys. Rev. B **51**, 7429 (1995).

5) D. S. Hirashima and T. Mutou, Physica B **199** & **200**, 206 (1994); T. Mutou and D. S. Hirashima, J. Phys. Soc. Jpn. **63**, 4475 (1994).

6) H. Tsunetsugu, Y. Hatsugai, K. Ueda, and M. Sigrist, Phys. Rev. B **46**, 3175 (1992).

7) A. M. Tsuvelik, Phys. Rev. Lett. **72**, 1048 (1994).

8) N. Shibata, T. Nishino, K. Ueda, and C. Ishii, Phys. Rev. B **53**, R8828 (1996).

9) K. Itai and P. Fazekas, Phys. Rev. B **54**, R752 (1996).

10) A. Georges, G. Kotliar, W. Krauth, and M. J. Rozenberg, Rev. Mod. Phys. **68**, 13 (1996); G. Kotliar, S. Y. Savrasov, K. Haule, V. S. Oudovenko, O. Parcollet, and C. A. Marianetti, Rev. Mod. Phys. **78**, 865 (2006).

11) X. Y. Zhang, M. Rozenberg, and G. Kotliar, Phys. Rev. Lett. **70**, 1666 (1993).

12) E. Nagira, S. Fujita, and T. Mutou, J. Phys. Soc. Jpn. **83**, 124710 (2014).

13) T. Schork and S. Blawid, Phys. Rev. B **56**, 6559 (1997).

14) R. Sato, T. Ohashi, A. Koga, and N. Kawakami, J. Phys. Soc. Jpn. **73**, 1864 (2004).

15) A. Koga, N. Kawakami, R. Peters, and Th. Pruschke, Phys. Rev. B **77**, 045120 (2008).

16) T. Yoshida, T. Ohashi, and N. Kawakami, J. Phys. Soc. Jpn. **80**, 064710 (2011).

17) I. Hagymási, K. Itai, and J. Sólyom, Phys. Rev. B **85**, 235116 (2012).

18) J. M. Luttinger, Phys. Rev. **119**, 1153 (1960); J. M. Luttinger and J. C. Ward, Phys. Rev. **118**, 1417 (1960); R. M. Martin, Phys. Rev. Lett. **48**, 362 (1982).

19) W. Metzner and D. Vollhardt, Phys. Rev. Lett. **62**, 324 (1989).

20) A. Georges and W. Krauth, Phys. Rev. B **48**, 7167 (1993).